

COMPARATIVE TRANSCRIPTOME ANALYSIS OF THE KEY GENES ASSOCIATED WITH THE ACCUMULATION OF LYCORINE AND GLANTHAMINE IN *LYCORIS AUREA*

XIAOLIANG XIANG, XIA JIANG¹, ZHAOTUN HU, JIUXIN TANG
AND MIAOHUA QUAN*

Key Laboratory of Research and Utilization of Ethnomedicinal Plant Resources of Hunan Province, College of Biological and Food Engineering, Huaihua University, Huaihua, P. R. China

Keywords: Lycoris aurea, Transcriptome, RNA sequencing, Lycorine, Glanthamine

Abstract

Lycoris aurea (*L. aurea*) can synthesize secondary metabolites, known as lycorine and galanthamine. Despite its pharmaceutical significance, the molecular mechanism underlying the accumulation of these medicinal components in *L. aurea* remains largely unexplored. Two populations of *L. aurea* (Hunan and Guangxi) with different contents of lycorine and galanthamine were selected for de novo RNA sequencing. A total of 337,746 unigenes were obtained, and 55,910 unigenes were differentially expressed between the two populations, consisting of 38,429 up-regulated and 17,481 down-regulated unigenes. Furthermore, expression pattern analysis showed that there were five differentially expressed genes involved in the biosynthesis of lycorine and galanthamine. Among them, tyrosine decarboxylase was significantly up-regulated, and it might be responsible for the differential accumulation of lycorine and galanthamine in different populations of *L. aurea*. Our findings provided new insights into the mechanism underlying the accumulation of lycorine and galanthamine, enriching the genetic resources for *L. aurea* breeding programs.

Introduction

Lycoris aurea (L' Hér.) Herb., also called Golden Magic Lily, belonging to *Amaryllidaceae* family, is one of the important perennial herbs in the genus *Lycoris* (Ma *et al.* 2016, Quan and Liang 2017). The bulbs of *L. aurea* have long been used in traditional Chinese medicine (TCM) (Song *et al.* 2014). Several types of secondary metabolites, known as *Amaryllidaceae* alkaloids, isolated from the bulbs of *L. aurea* have been reported to exhibit a wide spectrum of biological activities (Liao *et al.* 2012, Guo *et al.* 2014, Jin *et al.* 2014 and Song *et al.* 2014). For example, lycorine, a natural alkaloid extracted from *Amaryllidaceae* plant family, has been reported to exhibit various beneficial biological activities, such as anti-inflammation, anti-cancer, anti-viral and anti-malarial activities (Toriizuka *et al.* 2008, Liu *et al.* 2011, Kang *et al.* 2012, Chen *et al.* 2015 and Sun *et al.* 2018). As an *Acetylcholinesterase* inhibitor, galanthamine, another major *Amaryllidaceae* alkaloid, has also been used for the treatment of Alzheimer's disease (Rizzi *et al.* 1999, Bartolucci *et al.* 2001). Therefore, *L. aurea* has important medicinal value and broad application prospects.

Despite the medicinal and economic importance of *L. aurea*, our understanding of the mechanism underlying the accumulation of active alkaloid components has been limited due to the lack of genomic resources. In recent years, several types of transcriptome sequencing platforms have been used for discovering genes related to secondary metabolism in *L. aurea* (Wang *et al.* 2013, Wang *et al.* 2016 and Xu *et al.* 2016). However, those previous RNA-seq studies have focused only on the developmental stages or tissue types of one specific population, while studies

*Author for correspondence: <hhqmh100@163.com>.¹College of Chemistry and Materials Engineering, Huaihua University, Huaihua, Hunan, P. R. China.

focusing on different populations with diverse contents of bioactive components have not been conducted.

In the present study, two different *L. aurea* populations (Hunan and Guangxi) were selected. We found that the contents of lycorine and galanthamine in Guangxi population were significantly higher than those in Hunan population. Moreover, Illumina RNA-Seq was used to investigate the transcriptome profile of these two populations in order to unravel the differentially expressed genes (DEGs) involved in biosynthetic pathway of lycorine and galanthamine. Collectively, the findings in our current study would expand our understanding of the biosynthetic and regulatory mechanisms of lycorine and galanthamine in *L. aurea*, enriching the genetic resources for *L. aurea* breeding.

Materials and Methods

Two wild populations of *L. aurea*, designated as Guangxi and Hunan, were used to construct *L. aurea* transcriptomes. The Guangxi population was collected from Guilin City, Guangxi Province, China, while the Hunan population was collected from Huaihua City, Hunan Province, China. *L. aurea* plants were grown with appropriate irrigation and fertilization under open-field conditions at Botanical Garden, Huaihua University, Hunan Province, China. The coordinates of the geographical location are 110°01' E, 27°35' N, and the climate in this location belongs to *humid* or *monsoon subtropical* climate. In April 2017, the bulbs of *L. aurea* were dissected from the plants, washed with sterile water, immediately frozen in liquid nitrogen and stored at -80 °C prior to further analysis.

Extraction and quantification of lycorine and galanthamine from bulb tissues of *L. aurea* were carried out essentially according to a previously described method (Quan and Liang 2017). The collected bulbs were dried at 65°C to constant weights and then ground into a fine powder, and 2 g powder was extracted with 100 ml methanol in a water bath at 80°C for 3 hrs and then filtered. The filtrate was dried in a rotary evaporator under vacuum. The residue was then dissolved in 10 ml of 2.0% hydrochloric acid. The mixture was filtered, and the filtrate was adjusted to pH 10.0 by adding ammonia and then extracted three times with chloroform (15 ml for each). The collected chloroform solutions were combined and dried with a rotary evaporator. The residue was dissolved in 25 ml methanol and analyzed by HPLC after filtration through a 0.22 µm membrane. HPLC analysis was performed on Waters system (Waters, Avondale, CA) equipped with a Waters binary 1525 pump and a Waters 2489 UV/visible detector. The chromatographic separation was performed on a Waters X Select HSST3C18 column (5 µm, 4.6 × 250 mm). The mobile phase consisted of 0.1% phosphoric acid in water (A) and methanol (B). The gradient elution was programmed as follows: 5-20% B at 0-10 min, 20-40% B at 10-30 min, 40-80% B at 30-50 min, and 80-100% B at 50-56 min. Column temperature was maintained constant at 25°C, and the injection volume was 20 µL. The flow rate was set at 1.0 ml/min. The detection wavelength was set at 288 nm. The average contents of lycorine and galanthamine were calculated and defined as the milligram of alkaloid per one gram dried tissue, and at least three independent samples of each tissue were used. Data were expressed as means ± standard deviation (SD) of all replicates.

Total RNA of the two populations were extracted from 2 g bulb tissue samples using the TRIzol reagent according to the manufacturer's instructions (Life Technologies). Briefly, the polyA+ mRNA in the total mRNA was isolated using RNA Purification Beads (NEB). The mRNA libraries were constructed using the NEBNext® Ultra RNA Library Prep Kit for Illumina® protocol (NEB). Finally, the RNA-seq library was sequenced using an Illumina HiSeq X Ten sequencing platform at Chi-Biotech Co., Ltd., Shenzhen, China. The high-quality reads that passed the Illumina filter were subjected to the subsequent bioinformatics analysis.

The raw sequencing reads from transcriptome libraries were processed to get clean reads by removing the adapter sequences and low-quality reads. Filtration and quality control checks of the raw reads from RNA-seq were conducted by FastQC. After obtaining clean reads, de novo transcriptome assembly was performed using Trinity program (trinityrnaseq-2.2.0), which is based on the de Bruijn graph algorithm (Grabherr *et al.* 2011).

The assembled non-redundant transcripts from Hunan and Guangxi populations were merged and used as reference sequences. Then reads were mapped to transcripts using the hyper-accurate mapping algorithm FANSe2 in the NGS analysis platform “Chi-Cloud” (<http://www.chi-biotech.com>) (Xiao *et al.* 2014). Candidate coding regions were identified by TransDecoder and then annotated with non-redundant protein (NR), non-redundant nucleotide (NT), Clusters of Orthologous Groups of proteins (KOG/COG), Swiss-Prot, GO, Protein family (Pfam) and KEGG databases, respectively

Gene expressions were examined using the RPKM method (Mortazavi *et al.* 2008). Genes with at least 10 reads were considered as quantifiable genes (Bloom *et al.* 2009). The R statistical package software edgeR (version 3.12.0) was used to quantify the expressions of DEGs (Robinson *et al.* 2010). Moreover, $\log_2FC > 1$ and p value < 0.01 were used to identify significant differences in transcript expression. Functional enrichment analysis including GO and KEGG pathways were performed using topGO (version 2.22.0) (Alexa *et al.* 2006) and KOBAS (version 2.0) (Xie *et al.* 2011) for the identified DEGs, respectively.

TYDC, the expression of putative gene involved in lycorine and galanthamine biosynthesis was determined via qRT-PCR. The qRT-PCR protocol was performed as described by Wang *et al.* (Wang *et al.* 2019). Oligonucleotide primers used in this study were as follows: TYDC primers: forward, 5'-CTGCGAGAGACAGGGTACTGAATA-3', and reverse, 5'-CACCTTTTGTAGCTCCTCAGGATT-3'. TIP41 primers: forward, 5'-GCAACCATCCAAAGTTTAACTGCT-3', and reverse, 5'-AATGTGCAAGCAGGGCTAGTAA-3'.

Statistical analysis was performed using GraphPad Prism 5.0, and differences were analyzed with *t*-test. Statistical significance was assumed at $p < 0.05$.

Results and Discussion

The bulbs of Hunan and Guangxi populations have significantly different contents of lycorine and galanthamine. To elucidate the molecular and genetic mechanisms of main medicinal components accumulated in *L. aurea*, two *L. aurea* populations (Hunan and Guangxi populations) were selected for comparative analysis of gene expression. Fig. 1A shows that Hunan population and Guangxi population were two closely related populations with very similar morphological characters. The major active components of *L. aurea* are *Amaryllidaceae* alkaloids, such as lycorine and galanthamine (Fig. 1B). To ensure that the two populations under investigation had striking difference in accumulation of main medicinal components, the lycorine and galanthamine contents of Hunan and Guangxi bulbs were determined via high-performance liquid chromatography (HPLC) (Fig. 1B, C). Results indicated that Guangxi population contained relatively higher levels of *Amaryllidaceae* alkaloids, with 1.32 ± 0.18 mg/g lycorine and 0.23 ± 0.02 mg/g galanthamine, whereas the contents of lycorine and galanthamine in Hunan population were 0.22 ± 0.02 mg/g and 0.05 ± 0.01 mg/g, respectively (Fig. 1D). Considering that the secondary metabolites would plausibly be influenced by the environment (Jay-Allemand *et al.* 2015), two populations used in this study were grown under the same environmental conditions for more than 3 years. Therefore, we could conclude that the difference in the accumulation of galanthamine and lycorine between the two populations was attributed to their genetic backgrounds. Moreover, developing genomic resources and further research on the genetic

diversity and medicinal components accumulation relationship of the *L. aurea* will provide valuable information that can be used for better germplasm utilization and breeding innovation of *L. aurea*.

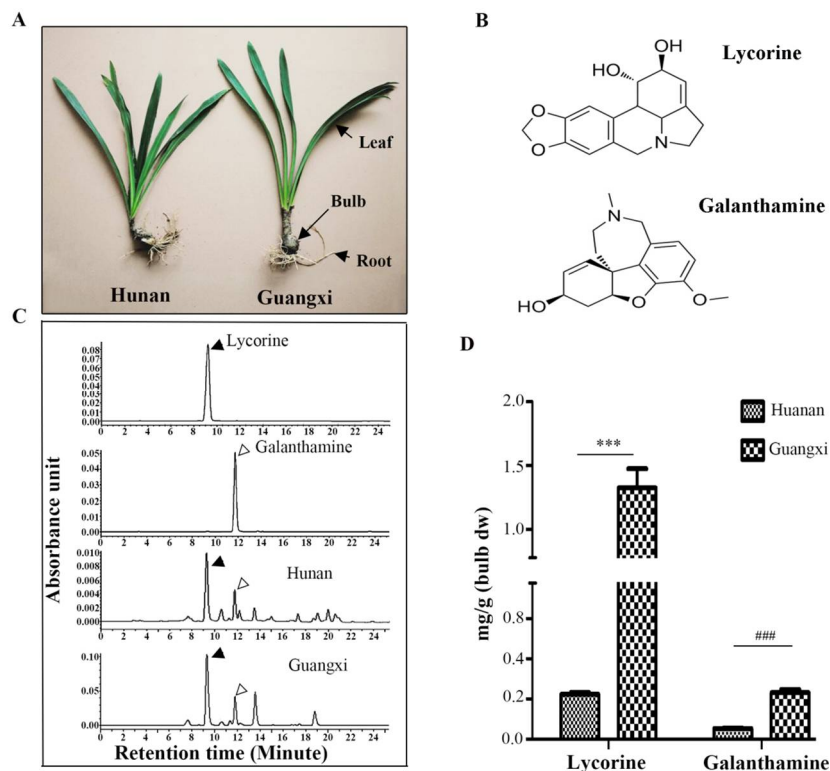


Fig. 1A-D: Differential biosynthesis of lycorine and galanthamine in bulb tissues of two *L. aurea* populations. A. Phenotypes of two populations (Hunan and Guangxi). B. Chemical structures of lycorine and galanthamine. C. Representative HPLC profiles of Hunan and Guangxi populations. D. The contents of lycorine and galanthamine in two *L. aurea* populations.

The sequencing of *L. aurea* cDNA libraries generated 64,442,420 and 29,144,078 raw reads from Hunan and Guangxi populations, respectively. By filtering all the raw reads, we obtained 53,891,177 (83.63%) clean reads from Hunan population and 29,144,078 (82.67%) from Guangxi population. Furthermore, high-quality reads from two populations were assembled de novo using Trinity, resulting in 388,488 transcripts. These transcripts were classified into 337,746 unigenes. The average contig length was 391.46 bp, and the contig N50 was 389. Table 1 summarizes the statistical analysis of data. Therefore, the obtained transcriptome assembly was used for further annotation and characterization.

Population variation in contents of medicinal components may be attributed to the differential expressions of genes. Fig. 2 shows the scatter plot, in which global gene expression profiles of the two populations were compared. The expression variation was the largest between the two populations. The gene expressions were determined based on the reads per kilobase per million (RPKM) values of assembled unigenes to identify the up-regulated and down-regulated genes between the two populations (Fig. 3A). The distribution of RPKM values revealed that the

expression pattern in Hunan population was different from that in Guangxi population. Fig. 3B exhibits the distribution profile of genes expressed in both populations. Based on the applied thresholds, \log_2 fold-change (\log_2FC) > 1 and p value < 0.01 , we found 55,910 DEGs. Comparing the population of Guangxi to the population of Hunan, 38,429 of these DEGs were downregulated and 17,481 were upregulated. Furthermore, comparative analysis of the transcriptomes of the two populations are needed to better understand the molecular mechanism underlying the accumulation of galanthamine and lycorine in *L. aurea*.

Table 1. Summary of assembly and annotation results for Hunan population and Guangxi population using Trinity

	Hunan population	Guangxi population
Total number of reads	64,442,420	35,254,345
Mapped reads	53,891,177	29,144,078
Mapping rate	83.63%	82.67%
Total trinity transcripts	388,488	
Unigenes	337,746	
Average contig length	391.46	
Contig N50	389	

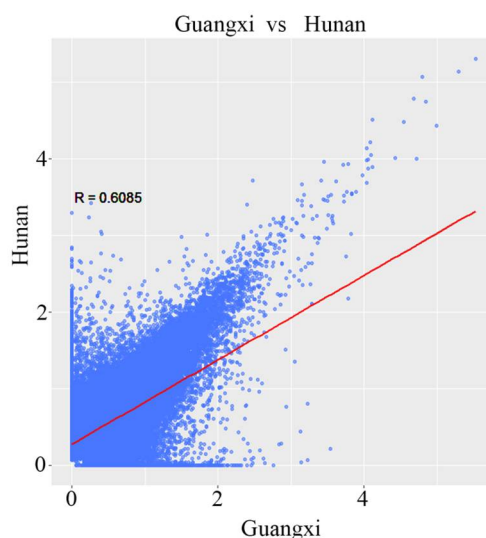


Fig. 2. Correlation analysis of gene transcription profiles between Hunan and Guangxi populations. The determine coefficient (R) is indicated in the figure.

In order to further reveal the possible function of DEGs between the two populations, we applied functional enrichment based on the Gene Ontology (GO) classification (Fig 4). The functions of these DEGs were categorized into three categories, namely biological process, cellular component and molecular function. On the basis of sequence homology, DEGs annotated in the GO database were further categorized into 60 functional groups. In addition, “single-organism metabolic process”, “small molecule metabolic process” and “oxidation-reduction

process” were dominant within the “biological process” category; “membrane”, “membrane part”, “intrinsic component of membrane” and “integral component of membrane” were dominant within the “cellular component” category; and “catalytic activity” predominated the “molecular function” category. The DEGs coding for these physiological processes might affect the accumulation of lycorine and glathamine in *L. aurea*.

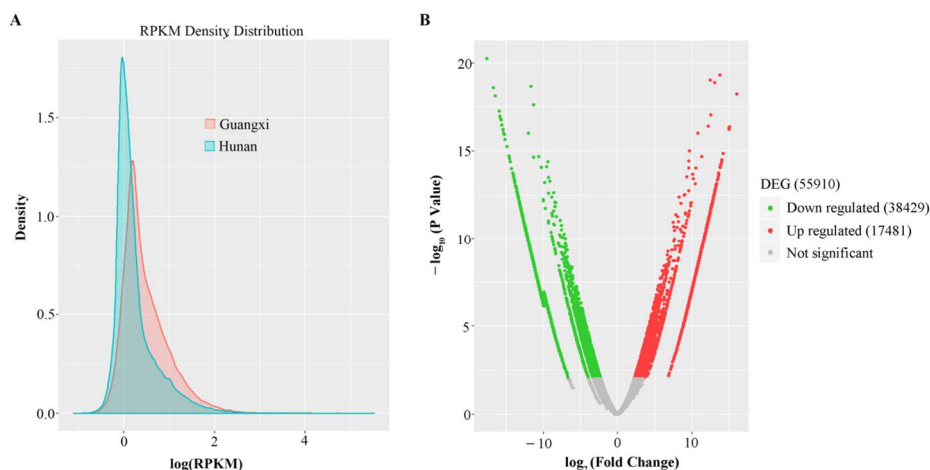


Fig. 3. Comparison of expression patterns of DEGs identified between Hunan and Guangxi populations. A. Frequency distribution of Hunan and Guangxi populations by RPKM. B. DEGs in two populations of *L. aurea*. The red dots represent up-regulated DEGs, the green dots represent down-regulated DEGs, and the gray dots represent non-DEGs. A total of 55,910 unigenes were identified as DEGs (p value < 0.01 and $\log_2FC > 1$) between Guangxi and Hunan populations.

Identification and functional analysis of the candidate DEGs related to specialized metabolic pathways could be extremely useful to understand the molecular and biochemical basis for the accumulation of such highly medicinally active metabolites in *L. aurea* (Wang *et al.* 2016). To further understand the biochemical pathways of these DEGs, we mapped them to terms in the Kyoto Encyclopedia of Genes and Genomes (KEGG) database (Kanehisa and Goto 2000) and compared these results with the complete transcriptome background. Fig. 5 shows a scatter plot of the DEGs that were enriched in the top 20 KEGG pathways. The three most significantly enriched pathways among these were "glyoxylate and dicarboxylate metabolism" (P value 0.000667479), "alanine, aspartate, and glutamate metabolism" (P value 0.001596665), and "two-component system" (P value 0.001987719).

The major medicinal ingredients (galanthamine and lycorine) in *L. aurea* belong to isoquinoline alkaloids (Markmee *et al.* 2006 and Swaffar *et al.* 2012). In order to find pivotal candidate genes responsible for the difference in accumulation of galanthamine and lycorine, we surveyed DEGs in *L. aurea* involved in the biosynthetic pathway of isoquinoline alkaloids (http://www.kegg.jp/kegg-bin/show_pathway?map00950). After KEGG annotation for all unigenes, 23 unigenes were found to be involved in the biosynthetic pathway of isoquinoline alkaloids. Moreover, five DEGs were identified in this pathway. These five DEGs belonged to five enzymes (tyrosine decarboxylase, EC:4.1.1.25; aspartate aminotransferase, mitochondrial, EC:2.6.1.1; polyphenol oxidase, EC:1.10.3.1; monoamine oxidase, EC:1.4.3.4; primary-amine oxidase, EC:1.4.3.21) (Fig. 6A). Interestingly, among these five DEGs, only one DEG, tyrosine

decarboxylase (TYDC), was up-regulated in Guangxi population, which also had the higher contents of lycorine and glanthamine. qRT-PCR analysis showed that TYDC has the same expression trends as it in RNA-seq data (Fig. 6B).

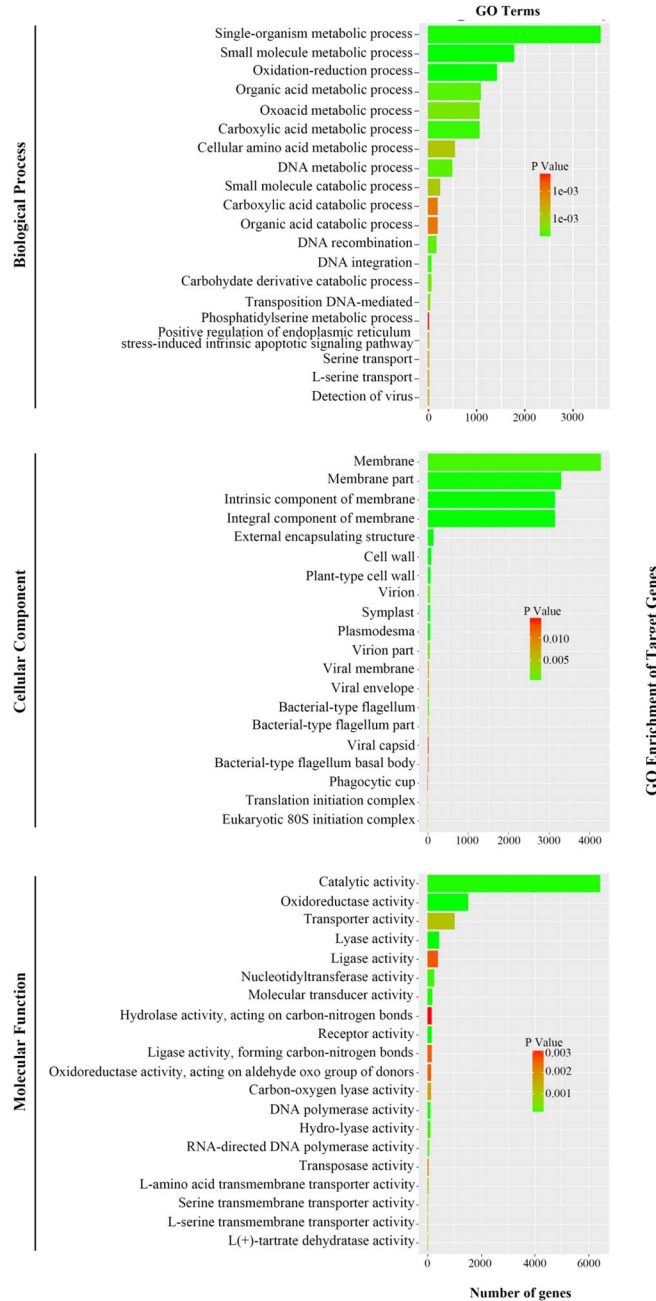


Fig. 4. Histogram of GO classification. The DEGs were summarized in three main categories, biological process, cellular component and molecular function.

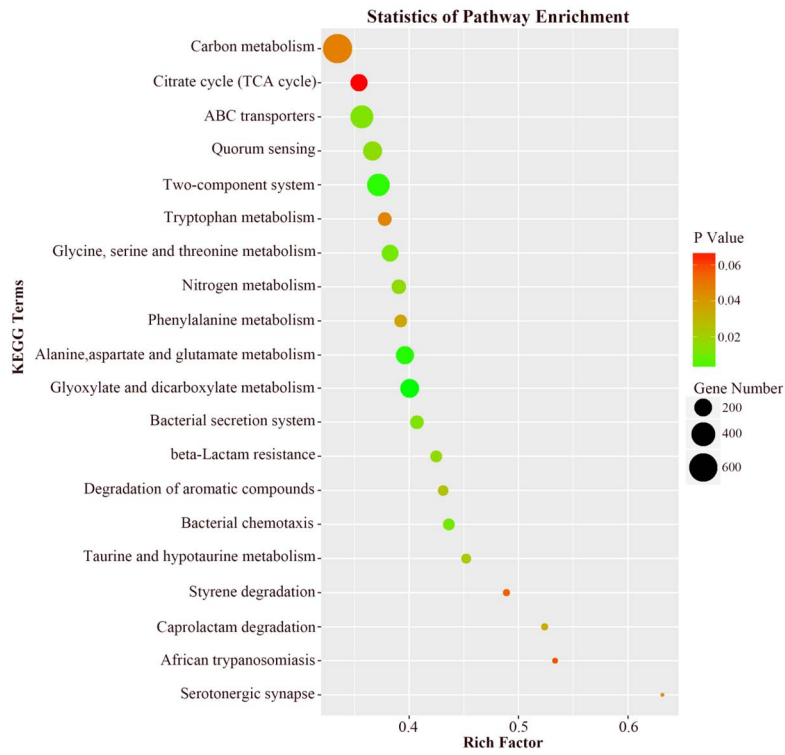


Fig. 5. Scatter plot of DSGs enriched in the top 20 KEGG pathways. Rich factor represents the ratios of the number of DEGs and the number of all unigenes in the pathway. Size of dot represents number of DEGs in the pathway. Dot color corresponds to scope of corrected p value.

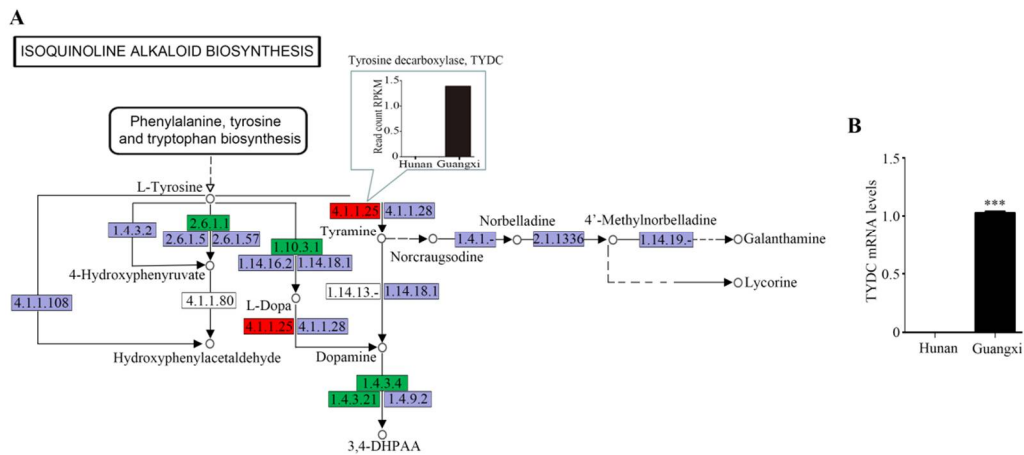


Fig. 6. The DEGs related to biosynthetic pathway of isoquinoline alkaloid.

A. Circles indicate chemical components, rectangles are enzymes with the given EC numbers, arrows are direction of reaction, and dotted arrows are indirection of reaction. Note: the red frames represent up-regulated DEGs in Guangxi population, the green frames represent down-regulated DEGs in Guangxi population, and the purple frames represent non-DEGs. B. TYDC transcript level was determined by qRT-PCR analysis. Data are presented as the mean (\pm SE) of three biological replicates.

Isoquinoline alkaloids are L-tyrosine-derived plant alkaloids with an isoquinoline skeleton. The L-tyrosine is first transformed to tyramine, which serves as distant precursors to isoquinoline alkaloids and as immediate precursors to lycorine and galanthamine (Diamond and Desgagne-Penix 2016). As the first key enzyme on this pathway, TYDC is a common cyclic amino acid in plants. In different plant species, it catalyzes the conversion of L-tyrosine and L-dopa to tyramine and dopamine, representing the first step in biosynthesis of a large and diverse group of plant secondary metabolites derived from tyrosine (Kim *et al.* 2011, Yang *et al.* 2018). Evidence suggests that over-expression of TYDC in medicinal plant opium poppy can increase the biosynthesis of isoquinoline alkaloids (Facchini and De Luca 1995). It was noteworthy that the expressions of enzymes involved in the tyrosine metabolic pathway, such as aspartate aminotransferase, polyphenol oxidase, monoamine oxidase, and primary-amine, were all down-regulated in Guangxi population. These results indicated that the isoquinoline alkaloid pathway was more conducive to production of galanthamine and lycorine in Guangxi population. Therefore, we concluded that TYDC plays a decisive role in driving the biosynthesis of lycorine and galanthamine in *L. aurea*.

Transcriptome sequencing analysis is a powerful method for gene discovery in biosynthesis of plant natural products from different non-model medicinal plants, in which no reference genome is available (Han *et al.* 2016). In the present study, two *L. aurea* populations with different contents of bioactive metabolites were selected to analyze the biosynthesis of lycorine and galanthamine using RNA-seq. We adopted Illumina technology to analyze the transcriptomes in the bulbs of two *L. aurea* populations, and characterized them by *de novo* assemble, functional annotation and comparative analysis. We built the high-quality transcripts and unigenes for *L. aurea*. A total of 388,488 transcripts were obtained from two *L. aurea* populations, and the resulting 337,746 unigenes were assembled, which could effectively fill a gap in the public databases of *L. aurea* transcriptome. Additionally, 55,910 unigenes were significantly differentially expressed between the two study populations by statistical analysis of RPKM. To reveal the genes involved in the biosynthetic accumulation of lycorine and galanthamine in *L. aurea*, differential analyses of the transcriptome revealed that TYDC might be used as a pivotal candidate enzyme responsible for the differential accumulation of lycorine and galanthamine in various *L. aurea* populations.

Collectively, our comprehensive study revealed a key enzyme in the production of main bioactive metabolites of *L. aurea*. Our findings provided valuable insights into further in-deep investigation of the regulatory mechanism underlying the accumulation of essential medicinal compounds in *L. aurea*.

Acknowledgements

This work was financially supported by the National Natural Science Foundation of China (No.32070367, No. 31470403, No.31900705), Science and Technology Innovation Program of Huaihua City (No.2021R3132), Hunan Innovation and Entrepreneurship Training project for College Students (No.S201910548027, No.S202010548001), Science and Technology Innovation Program of Hunan Province (No.2020RC1013, 2021RC1015), and Foundation of Hunan Double First-rate Discipline Construction Projects of Bioengineering (No.YYZW2019-15, No. YYZW2019-25).

References

Alexa A, Rahnenfuhrer J and Lengauer T 2006. Improved scoring of functional groups from gene expression data by decorrelating GO graph structure. *Bioinformatics*. **22**: 1600-1607.

- Bartolucci C, Perola E, Pilger C, Fels G and Lamba D 2001. Three-dimensional structure of a complex of galanthamine (Nivalin) with acetylcholinesterase from *Torpedo californica*: implications for the design of new anti-Alzheimer drugs. *Proteins*. **42**: 182-191.
- Bloom J, Khan SZ, Kruglyak L, Singh M and Caudy AA 2009. Measuring differential gene expression by short read sequencing: quantitative comparison to 2-channel gene expression microarrays. *BMC Genomics*. **10**: 221-230.
- Chen DZ, Cai JY, Yin JL, Jiang JD and Jing CX 2015. Lycorine-derived phenanthridine downregulators of host Hsc70 as potential hepatitis C virus inhibitors. *Future Med. Chem.* **7**: 561-570.
- Diamond A and Desgagne PI 2016. Metabolic engineering for the production of plant isoquinoline alkaloids. *Plant Biotechnol.* **14**: 1319-1328.
- Facchini PJ, and De Luca V 1995. Phloem-Specific Expression of Tyrosine/Dopa Decarboxylase Genes and the Biosynthesis of Isoquinoline Alkaloids in Opium Poppy. *Plant Cell*. **7**: 1811-1821.
- Grabherr MG, Haas BJ, Yassour M, Levin JZ, Thompson DA, Amit I, Adiconis X, Fan L, Raychowdhury R and Zeng Q 2011. Full-length transcriptome assembly from RNA-Seq data without a reference genome. *Nat. Biotechnol.* **29**: 644-652.
- Guo Y, Pigni NB, Zheng YH, de Andrade JP, Torras-Claveria L, de Souza Borges W, Viladomat F, Condina C and Bastida J 2014. Analysis of bioactive Amaryllidaceae alkaloid profiles in *Lycoris* species by GC-MS. *Nat. Prod. Commun.* **9**: 1081-1086.
- Han R, Rai A, Nakamura M, Suzuki H, Takahashi H, Yamazaki M and Saito K 2016. De Novo Deep Transcriptome Analysis of Medicinal Plants for Gene Discovery in Biosynthesis of Plant Natural Products. *Methods Enzymol.* **576**: 19-45.
- Jay-Allemand C, Tattini M and Gould 2015. New evidence for the functional roles of secondary metabolites in plant-environment interactions. *Environ. Exp. Bot.* **119**: 1-3.
- Jin A, Li X, Zhu YY, Yu HY, Pi HF, Zhang P and Ruan HL 2014. Four new compounds from the bulbs of *Lycoris aurea* with neuroprotective effects against CoCl_2 and H_2O_2 -induced SH-SY5Y cell injuries. *Arch. Pharm. Res.* **37**: 315-323.
- Kanehisa M and Goto S 2000. KEGG: kyoto encyclopedia of genes and genomes. *Nucleic acids res.* **28**: 27-30.
- Kang J, Zhang Y, Cao X, Fan J, Li G, Qi W, Diao Y, Zhao ZH, Luo L and Yin ZM 2012. Lycorine inhibits lipopolysaccharide-induced iNOS and COX-2 up-regulation in RAW264.7 cells through suppressing P38 and STATs activation and increases the survival rate of mice after LPS challenge. *Immunopharmacol.* **12**: 249-256.
- Kim YS, Park S, Kang K, Lee K and Back K 2011. Tyramine accumulation in rice cells caused a dwarf phenotype via reduced cell division. *Planta* **233**: 251-260.
- Liao N, Ao M, Zhang P and Yu L 2012. Extracts of *Lycoris aurea* induce apoptosis in murine sarcoma S180 cells. *Molecules* **17**: 3723-3735.
- Liu JN, Yang YJ, Xu YF, Ma CM, Qin C, Qin C and Zhang LF 2011. Lycorine reduces mortality of human enterovirus 71-infected mice by inhibiting virus replication. *Virol. J.* **8**: 483-491.
- Ma R, Xu S, Zhao YC, Xia B and Wang R 2016. Selection and Validation of Appropriate Reference Genes for Quantitative Real-Time PCR Analysis of Gene Expression in *Lycoris aurea*. *Front. Plant Sci.* **7**: 536-550.
- Markmee S, Ruchirawat S, Prachyawarakorn V, Ingkaninan K and Khorana N 2006. Isoquinoline derivatives as potential acetylcholinesterase inhibitors. *Bioorg. Med. Chem. Lett.* **16**: 2170-2172.
- Mortazavi A, Williams BA, McCue K, Schaeffer L and Wold B 2008. Mapping and quantifying mammalian transcriptomes by RNA-Seq. *Nat. Methods.* **5**: 621-628.
- Quan M, and Liang J 2017. The influences of four types of soil on the growth, physiological and biochemical characteristics of *Lycoris aurea* (L' Her.) Herb. *Sci. Rep.* **7**: 43284-43292.

- Rizzi A, Schuh R, Bruckner A, Cvitkovich B, Kremser L, Jordis U, Frohlich J, Kuenburg B and Czollner L 1999. Enantiomeric resolution of galanthamine and related drugs used in anti-Alzheimer therapy by means of capillary zone electrophoresis employing derivatized cyclodextrin selectors. *J. Chromatogr. B Biomed. Sci. Appl.* **730**: 167-175.
- Robinson MD, McCarthy DJ, and Smyth GK 2010. edgeR: a Bioconductor package for differential expression analysis of digital gene expression data. *Bioinformatics* **26**: 139-140.
- Song JH, Zhang L and Song Y 2014. Alkaloids from *Lycoris aurea* and their cytotoxicities against the head and neck squamous cell carcinoma. *Fitoterapia* **95**: 121-126.
- Sun Y, Wu P, Sun Y, Sharopov FS, Yang Q, Chen F, Wang P and Liang Z 2018. Lycorine possesses notable anticancer potentials in on-small cell lung carcinoma cells via blocking Wnt/beta-catenin signaling and epithelial-mesenchymal transition (EMT). *Biochem. Biophys. Res. Commun.* **495**: 911-921.
- Swaffar D, Holley C, Fitch R, Elkin K, Zhang C, Sturgill J, Jennifer M and Menachery M 2012. Phytochemical investigation and in vitro cytotoxic evaluation of alkaloids from *Abuta rufescens*. *Planta Med.* **78**: 230-232.
- Toriiizuka Y, Kinoshita E, Kogure N, Kitajima M, Ishiyama A, Otaguro K, Omura S S and Takayama H 2008. New lycorine-type alkaloid from *Lycoris traubii* and evaluation of antitrypanosomal and antimalarial activities of lycorine derivatives. *Bioorg. Med. Chem.* **16**: 10182-10189.
- Wang R, Xu S, Jiang YM, Jiang JW, Li XD, Liang LJ, He J, Peng F and Xia B 2013. De novo sequence assembly and characterization of *Lycoris aurea* transcriptome using GS FLX titanium platform of 454 pyrosequencing. *PLoS One.* **8**: e60449-60458.
- Wang R, Xu S, Wang N, Xia B, Jiang YM and Wang R 2016. Transcriptome Analysis of Secondary Metabolism Pathway, Transcription Factors, and Transporters in Response to Methyl Jasmonate in *Lycoris aurea*. *Front. Plant Sci.* **7**: 1971-1983.
- Wang R, Han XK, Xu S, Xia B, Jiang YM, Xue Y and Wang R 2019. Cloning and characterization of a tyrosine decarboxylase involved in the biosynthesis of galanthamine in *Lycoris aurea*. *Peer J.* **7**: e6729-6746.
- Xiao CL, Mai ZB, Lian XL, Zhong JY, Jin JJ, He QY and Zhang G 2014. FANSe2: a robust and cost-efficient alignment tool for quantitative next-generation sequencing applications. *PLoS One* **9**: e94250-94262.
- Xie C, Mao X, Huang J, Ding Y, Wu J, Dong S, Lei K, Ge G, Li C and Wei L 2011. KOBAS 2.0: a web server for annotation and identification of enriched pathways and diseases. *Nucleic Acids Res.* **39**: W316-322.
- Xu S, Jiang Y, Wang N, Xia B, Jiang Y, Li X, Zhang Z, Li Y and Wang R 2016. Identification and differential regulation of microRNAs in response to methyl jasmonate treatment in *Lycoris aurea* by deep sequencing. *BMC Genomics.* **17**: 789-803.
- Yang W, Peng T, Li T, Cen J and Wang J 2018. Tyramine and tyrosine decarboxylase gene contributes to the formation of cyanic blotches in the petals of pansy (*Viola x wittrockiana*). *Plant Physiol. Biochem.* **127**: 269-275.

(Manuscript received on 5 March, 2022; revised on 2 December, 2022)